Silica-supported Ti chloride tetrahydrofuranates, precursors of Ziegler–Natta catalysts

Kalaivani Seenivasan, Erik Gallo, Andrea Piovano, Jenny G. Vitillo, Anna Sommazzi, Silvia Bordiga, Carlo Lamberti, Pieter Glatzel, and Elena Groppo*

"Silica-supported Ti chloride tetrahydrofuranates, precursors of Ziegler-Natta catalysts"

Dalton Trans., **42** (2013) 12706-12713.

doi: 10.1039/c3dt50603g

Silica-supported Ti chloride tetrahydrofuranates, precursors of Ziegler-Natta catalysts

Kalaivani Seenivasan,[a] Erik Gallo,[a,b] Andrea Piovano,[c] Jenny G. Vitillo,[a] Anna Sommazzi,[d] Silvia Bordiga,[a] Carlo Lamberti,[a] Pieter Glatzel,[b] and Elena Groppo*[a]

The structural and electronic properties of silica-supported titanium chloride tetrahydrofuranates samples, obtained by impregnating a polymer-grade dehydroxylated silica with $TiCl_4(thf)_2$ and $TiCl_3(thf)_3$ complexes, precursors of Ziegler-Natta catalysts, are investigated by means of FT-IR, XAS, XES and diffuse reflectance UV-Vis spectroscopy, coupled with DFT calculations. The properties of the two silica-supported samples are very similar, irrespective of the starting precursor. In both cases, most of the chlorine ligands originally surrounding the Ti sites are substituted by oxygen ligands upon grafting on silica. As a consequence, the electronic properties of silica-supported Ti sites are largely different from those of the corresponding precursors, and in both cases most of the grafted Ti sites have a formal oxidation state of +4. The whole set of experimental data provide evidence that mono-nuclear Ti species are mainly present at the silica surface.

1. Introduction

Reactions of silica surface with organometallic species are of fundamental importance in many areas of chemistry, and in particular in heterogeneous catalysis.[1-6] Amorphous silica is widely used as a support for many heterogeneous catalysts, because of its high surface area, thermal and mechanical stability. In most of the cases, the active phase is formed upon reaction of the well defined organometallic precursors with surface silanol groups, whose concentration and type can be tuned by changing the temperature of the pre-treatments.[7] When the grafting procedure is performed on a highly dehydroxylated silica, the grafted metal species can assume a single-site character.[2-4,8] Several heterogeneous catalysts for olefin polymerization are supported on amorphous silica; the silica types involved are porous, with high specific surface areas and potentially reactive surface hydroxyl groups almost entirely upon the pore walls.[9] The first developed polyolefin catalyst based on silica was the Phillips catalyst for ethylene polymerization, where the active sites are diluted chromium centres.[10-12] In such a case it was demonstrated that silica does not play the role of an inert support only, but directly influences the properties of the grafted chromium species in terms of accessibility, coordination ability and flexibility.[10,11,13,14] Amorphous silica was successively employed as a support also for Ti-based Ziegler-Natta catalysts for ethylene polymerization.[9,15,16] The simple combination of titanium tetrachloride on silica yielded low-reactivity catalysts; however, the combination of a magnesium compound with a porous silica material, followed by reaction with titanium tetrachloride, resulted in a catalyst showing an enhanced reactivity and the excellent handling and polymer particle control characteristic of Phillips' chromium catalysts.[9,15,16] In contrast to chromium-based catalysts, the role of silica surface chemistry in Ziegler-Natta catalysts is often overlooked.

In the frame of a wider work devoted to the physical-chemical characterization of silica-supported Ziegler-Natta catalysts based on tetrahydrofuranates of $TiCl_4$ and $MgCl_2$,[17] we performed a detailed spectroscopic investigation on the reactivity of titanium chloride tetrahydrofuranates ($TiCl_4(thf)_2$ and $TiCl_3(thf)_3$, thf = tetrahydrofurane) towards a polymer-grade silica and on the structure of the resulting Ti-grafted sites. Reactivity of surface hydroxyl groups of silica towards titanium chloride and other metal chlorides was studied in the past by several research groups, mainly by FT-IR spectroscopy and chemical analysis, and was used as a mean of determining the surface structure and the number of isolated and H-bonded hydroxyl groups of silica.[18-23] In particular, IR studies demonstrated the occurrence of a dissociative chemisorption of $TiCl_4$ on dehydrated silica, although it was not shown conclusively whether the isolated or the H-bonded hydroxyl groups are the most reactive toward $TiCl_4$.[18-23] Formation of both mono-functional $\equiv SiO\text{-}TiCl_3$ and bi-functional $(\equiv SiO)_2\text{-}TiCl_2$ species was postulated, whose proportion depends mainly on the silica dehydration temperature and on the reaction temperature. Hydrochloric acid was found as by-product in all the cases, and in some cases chlorination of silica was also observed. A similar reactivity was reported for several organometallic complexes of general formula X_xML_n (where M = transition metal, X = halogen and L = ligand) that were found to react with surface silanols ≡SiOH of highly dehydroxylated silica to yield $\equiv SiOMX_{x-1}L_n$ species along with HX.[1,3,4,24-27] For tetrahedral X_xML_n complexes, the grafting process usually occurs without major changes in terms of structure and geometry of the grafted fragment, that is tetrahedral d^0 ML_4 complexes remain mostly tetrahedral upon grafting for a large range of metals.

The case of Ti chloride tetrahydrofuranate complexes discussed in the following is less straightforward for at least two reasons. First, the starting complexes are six-folded coordinated and are less reactive with respect to the pure metal chlorides due to the presence of the thf ligands. Secondly, the employed silica is not highly dehydroxylated and, being porous, contains a large amount of internal hydroxyl groups interacting with each other. Therefore, the number of possible structures resulting from the grafting of the Ti complexes is theoretically much larger than those hypothesized for $TiCl_4$ alone on highly dehydroxylated silica and also the two extreme possibilities of no-grafting or formation of multi-nuclear Ti species should be taken into

account. While the occurrence of Ti grafting through surface ≡SiOH groups can be easily demonstrated by FT-IR spectroscopy (by looking at the consumption of the IR absorption bands due to surface ≡SiOH groups), insight on the geometric and electronic structure of the grafted Ti sites can be obtained only by coupling many characterization techniques, such as X-ray Absorption Spectroscopy (XAS),[28] X-ray Emission Spectroscopy (XES)[29] and diffuse reflectance UV-Vis spectroscopy.[30]

2. Experimental

2.1 Materials

Davison sylopol silica 955 grade (surface area = 276 m^2/g, pore volume = 1.76 ml/g, average pore diameter = 266 Å, average particle size = 31 μm) was used as support, after a pre-treatment in air at 550°C for 8 hours, followed by a cooling step carried out in nitrogen atmosphere. $TiCl_4(thf)_2$ and $TiCl_3(thf)_3$ precursors were synthesized following the recipe reported elsewhere.[31,32] The Ti^{IV} and Ti^{III} chloride tetrahydrofuranates were dissolved in dry tetrahydrofurane (thf) and impregnated on dehydroxylated SiO_2 in controlled atmosphere, using Schlenk technique. In both cases, Ti loading was 2 wt%. The excess of the solvent was further removed by gently heating the sample up to ca. 60°C.

2.2 Techniques

X-ray Powder Diffraction patterns were collected with a PW3050/60 X'Pert PRO MPD diffractometer from PANalytical working in Debye-Scherrer geometry, using as source a Cu anode. The samples were measured as powders inside a 0.8 mm boron-silicate capillary sealed in inert atmosphere.

FT-IR spectra were acquired in transmission mode on a Bruker Vertex70 spectrophotometer, at a resolution of 2 cm^{-1}. The samples were measured in the form of self supporting pellets inside a quartz cell in controlled atmosphere. UV-Vis-NIR spectra were collected in Diffuse Reflectance mode on a Cary5000 Varian spectrophotometer. All the samples were measured in the powdered form inside a home-made cell having an optical window (suprasil quartz) and allowing to perform measurements in controlled atmosphere. Silica-supported samples were measured without dilution, whereas non-supported samples were diluted in teflon.

X-ray absorption (XAS) experiments at the Ti K-edge were performed at the BM23 beamline of the ESRF facility (Grenoble, F). The EXAFS spectra of the two reference sample were collected in transmission mode; whereas those of the silica-supported samples were collected in fluorescence. The EXAFS part of the spectra was collected up to 12 $Å^{-1}$ with a variable sampling step in energy, resulting in $\Delta k = 0.03$ $Å^{-1}$. For each sample, three equivalent EXAFS spectra were acquired and averaged before the data analysis. EXAFS data analysis was performed using the Athena and Arthemis softwares.[33] Phase and amplitudes were calculated by FEFF6.0 code.[34]

XES experiments were performed at beamline ID26 of the European Synchrotron Radiation Facility (ESRF, France). The incident energy (Ω) was selected by means of a pair of cryogenically cooled Si(311) single crystals (higher harmonics were suppressed by three Si mirrors operating in total reflection). The fluorescence photon energy (ω) was selected using an emission spectrometer working in vertical Rowland Geometry employing five Ge(331) spherically bent analyzer crystals of radius 1000 mm covering 70-110 degrees in the horizontal scattering plane. The emitted photons were detected using an avalanche photo-diode. The total energy bandwidth was 0.9 eV (as determined from the full width at half maximum of the elastically scattered peak). The background of the vtc-XES spectra, due to the $K\beta_{1,3}$ peak tail, was subtracted according to the procedure discussed in Ref. [35,36]. DFT calculations were performed within the one electron approximation using the ORCA 2008 code.[37] Details are given in Ref. [35] and SI. The beam size on the sample was approximately 0.8 mm horizontally and 0.2 mm vertically. For both XAS and vtc-XES experiments, the samples were measured in the form of self-supporting pellets prepared inside a glove-box and placed inside a home-made cell with kapton windows; before measurements, the cell was outgassed in order to remove the Ar, which absorbs most of the beam at this low energy. The two precursors were diluted in a paraffin.

3. Results and Discussion

The two SiO_2-supported samples investigated in this work were prepared by impregnating a dehydroxylated silica with a tetrahydrofurane (thf) solution of either $TiCl_4(thf)_2$ or $TiCl_3(thf)_3$ precursors (hereafter labelled Ti^{IV} and Ti^{III}), resulting in both cases into a Ti loading of 2 wt% (see Experimental section). The employed silica is a polymer-grade silica dehydroxylated at 550°C, therefore containing a non-negligible amount of interacting ≡SiOH groups. The XRPD patterns of both $TiCl_4(thf)_2/SiO_2$ and $TiCl_3(thf)_3/SiO_2$ (hereafter Ti^{IV}/SiO_2 and Ti^{III}/SiO_2) show only a broad peak centred around $2\theta = 21°$, due to the amorphous silica support (Figure S1). The absence of other diffraction peaks indicates that no crystalline domains are present (within the sensitivity of the technique).

FT-IR spectroscopy was used to evaluate the occurrence of Ti grafting, as already proposed in literature.[18-23] The FT-IR spectra of Ti^{IV}/SiO_2 and Ti^{III}/SiO_2 are compared to that of the bare SiO_2 support pre-activated at 550°C in Figure 1. The FT-IR spectrum of SiO_2 (light grey) shows several IR absorption bands in the ν(OH) region: the sharp band at 3746 cm^{-1} is due to isolated silanol groups, whereas the broad absorption band having two maxima around 3670 and 3550 cm^{-1} indicates the presence of nests of hydroxyl groups weakly interacting with each other,[38,39] as commonly found in porous silicas.[9] At lower wavenumber values, the spectrum is dominated by the intense Si-O vibrational modes of the framework (in the 1400–950 cm^{-1} and 850–770 cm^{-1} ranges) and by their overtone modes (in the 2100–1550 cm^{-1} range).[40]

The FT-IR spectra of the Ti^{IV}/SiO_2 and Ti^{III}/SiO_2 pre-catalysts (dark grey and black in Figure 1) differ from that of the bare SiO_2 in both ν(OH) and framework vibrational modes regions. In particular, the IR absorption bands of both isolated silanols and internal hydroxyl groups have a lower intensity than in the pure support (more evident after subtracting the spectrum of the bare silica, Figure 1b), proving that a fraction of the surface hydroxyl groups react with the Ti chloride tetrahydrofuranate precursors during the synthesis step. Simultaneously, a new IR absorption band appear around 925 cm^{-1}, well evident in a narrow frequency region of transparency (subtracted spectra are shown in Figure

1c). Similar IR absorption bands were previously observed upon gas-phase reaction of $TiCl_4$ with dehydrated silica and assigned to Si-O-Ti vibrations of bi-functional grafted $(\equiv SiO)_2$-$TiCl_2$ species.[19,20,22] In analogy with the chemistry of $TiCl_4$, it can be hypothesized that the two Ti precursors react with the surface hydroxyl groups at the silica surface during the synthesis in solution; likely, the HCl released as by-product remains in solution. Additional evidence that most of the chlorine ligands are lost as a consequence of Ti grafting is obtained by a FT-IR study of H_2O adsorption and reaction (Section S3 and Figure S2). H_2O is mainly physisorbed on both Ti^{IV}/SiO_2 and Ti^{III}/SiO_2 samples and almost no hydrolysis reaction occurs, as it would be expected in presence of exposed chlorine ligands.

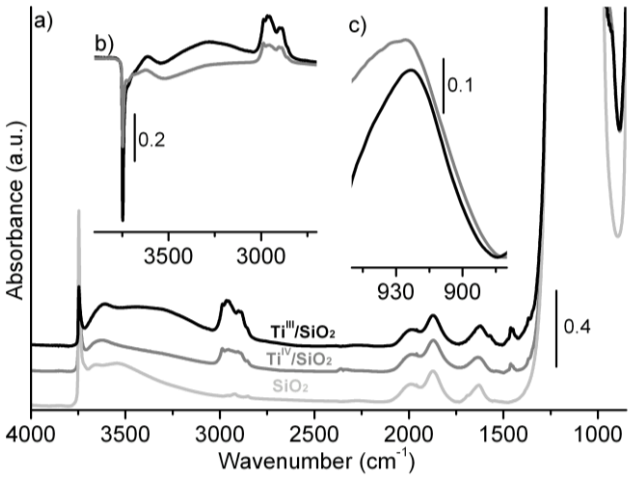

Fig. 1 Part a): FT-IR spectra (collected in inert atmosphere) of Ti^{IV}/SiO_2 (grey) and Ti^{III}/SiO_2 (black), compared to that of the SiO_2 support pre-activated at 550°C (light grey) (Ti^{IV}: $TiCl_4(thf)_2$; Ti^{III}: $TiCl_3(thf)_3$). The spectra have been normalized to the intensity of the absorption bands around 1900 cm^{-1} (first overtones of silica framework modes) in order to account for the thickness of the pellets, and a straight line was subtracted to better compare the spectra each others. Insets b) and c) show a magnification of the spectra of Ti^{IV}/SiO_2 and Ti^{III}/SiO_2 in 4000-2750 cm^{-1} and 950-850 cm^{-1} regions, after subtraction of the spectrum of bare SiO_2.

Finally, the IR spectra of both Ti^{IV}/SiO_2 and Ti^{III}/SiO_2 show IR absorption bands in the 3000-2800 cm^{-1} region ($\nu(CH_2)$ modes) and in the 1500-1350 cm^{-1} range ($\delta(CH_2)$ modes), testifying that thf molecules, or some species deriving from thf rearrangement,[41] are still present in the sample. However, it is difficult to verify whether thf is still attached to the Ti sites or is adsorbed on the silica support. In this regard, it should be noticed that independent FT-IR experiments of CO adsorbed at 100 K provide an evidence that the majority of grafted Ti sites do not have coordination vacancies available for CO insertion (Section S4 and Figure S3), suggesting that they retain the six-fold coordination geometry characteristic of the starting complexes. As a consequence, at least a fraction of the thf should be coordinated to the Ti sites.

In absence of any long-range order (see XRPD patterns in Figure S1), the local structure around the Ti atoms should be investigated by element selective spectroscopic techniques, such as Ti K-edge EXAFS. The potentiality of EXAFS in unravelling the local structure of the transition metal sites grafted on amorphous silica was largely demonstrated in the past.[1,2,13,28,42,43] Figure 2 shows the phase-uncorrected Fourier Transforms (FT) of the $k^3\chi(k)$ EXAFS functions for both Ti^{IV}/SiO_2 and Ti^{III}/SiO_2 (black spectra) in both modulus and imaginary parts (parts a and b, respectively). Also the EXAFS spectra of the corresponding $TiCl_4(thf)_2$ and $TiCl_3(thf)_3$ precursors are shown for comparison (gray spectra). Both Ti chloride tetrahydrofuranates complexes are molecular crystals; in each molecular unit, Ti atoms are six-fold coordinated to the same types of ligands (*i.e.* oxygen of the thf ring at around 2.0 Å and chlorine at around 2.3 Å), although in a different relative amount.[17] The similarity in the local structure of the two precursors explains why the corresponding EXAFS spectra are very similar to each others. They are dominated by a first shell signal centered around 1.8 Å (not corrected in phase), which is the result of the sum of the six single-scattering contributions deriving from the first shell ligands. Although the molecular structure of the two precursors is well known from XRPD, a quantitative analysis of the EXAFS signals was not possible within the available data quality because of the strong correlations among the fitted EXAFS variables.

The EXAFS spectra of the Ti^{IV}/SiO_2 and Ti^{III}/SiO_2 samples are different from those of the precursors, providing striking evidence that the two complexes are not simply physisorbed on the silica surface. In both cases, the |FT| is characterized by two main contributions, around 1.4 and 1.9 Å, respectively, whereas no signals are observed at longer distances. The spectra of Ti^{IV}/SiO_2 and Ti^{III}/SiO_2 are very similar to each other, although the relative intensity of the two contributions is slightly different in the two cases. As discussed for the reference compounds, a quantitative analysis of the EXAFS data of Ti^{IV}/SiO_2 and Ti^{III}/SiO_2 samples was affected by the strong correlation among the fitted variables and thus is not reliable. Nevertheless, a series of fits was performed by changing in a systematic way the relative number of oxygen and chlorine ligands. In such a way we introduced arbitrary constrains that significantly reduced the correlation among the remining parameters. The results are discussed in Section S5 and summarized in Tables S1 and S2. Contrarily to many successful examples in literature where EXAFS is used to determine the local structure around the absorbing metal species, in the present case we can use the EXAFS data only to conclude that the ligand sphere around the Ti sites contains more oxygen (contributing to the first shell peak) and less chlorine ligands (responsible of the contribution around 1.9 Å, not corrected in phase) than in the corresponding Ti^{IV} and Ti^{III} precursors. This finding is in agreement with the hypothesis that the Ti chloride tetrahydrofuranates complexes do graft to the silica surface via elimination of HCl. Finally, the absence of any signal at longer distances suggests that mono-nuclear Ti species are mainly present at the silica surface.

Since EXAFS spectroscopy was not conclusive to investigate the local structure around the Ti sites, we turned to valence-to-core X-ray emission spectroscopy (vtc-XES), which has been proved to be effective in the identification of the metal-ligand environment also when, contrary to XAS, the atomic number of the ligands is very close (*e.g.* XES can distinguish between O, N and C ligands).[44-46] vtc-XES is a second order optical process. For a 3d-transition metal, it can be induced by the absorption of an X-ray photon with energy higher than the 1s photo-excitation threshold; the so formed core hole is then filled by a valence electron lying below the Fermi level.[35,36,47] Note that the vtc-XES

features reflect the valence band density of occupied electronic states projected onto Ti *p* orbital angular momentum; thus, molecular orbitals with no metal *p* contribution cannot be detected. [35,36]

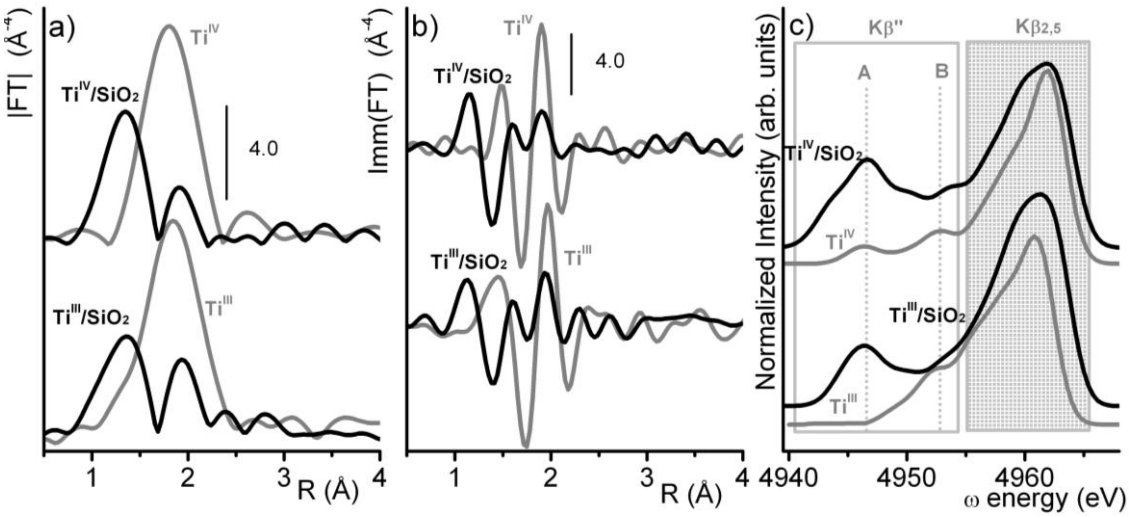

Fig. 2 Part a): Phase-uncorrected |FT| of the $k^3\chi(k)$ EXAFS function for Ti^{IV}/SiO_2 and Ti^{III}/SiO_2 (black). The EXAFS spectra of the two Ti chloride tetrahydrofuranates precursors are shown for comparison (grey). The spectra were extracted in the $\Delta k = 2.0 – 10.5$ Å^{-1} range. The spectra have been vertically translated for clarity. Part b): same as part a) for the Imm(FT). Part c): vtc-XES spectra of Ti^{IV}/SiO_2 and Ti^{III}/SiO_2 (black) and of the corresponding Ti^{IV} and Ti^{III} precursors (grey). The spectra have been vertically translated for clarity. The Kβ" and $K\beta_{2,5}$ regions are indicated with white and grey boxes, respectively. A and B features identify oxygen and chlorine ligands, respectively. Ti^{IV}: $TiCl_4(thf)_2$; Ti^{III}: $TiCl_3(thf)_3$.

Figure 2c shows the vtc-XES of both Ti^{IV}/SiO_2 and Ti^{III}/SiO_2, compared to those of the corresponding Ti^{IV} and Ti^{III} precursors. Two main regions can be in general identified in a vtc-XES spectrum, which are called Kβ" and $K\beta_{2,5}$ (white and grey boxes in Figure 2c, respectively). The Kβ" fluorescence lines are mainly due to transitions involving molecular orbitals (MOs) with ligands *s*-atomic character. They can be used for ligand identification.[35,36,44-46,48-50] Two Kβ" lines are present in the vtc-XES spectrum of Ti^{IV} precursor (A and B in Figure 2c). According to previous works on Ti compounds,[35,44] A and B are related to transitions involving MOs having primarily O(2s) and Cl(2p) character, respectively; hence, they identify the presence of oxygen and chlorine ligands in the first coordination sphere of the Ti sites. Feature A is not observed in the vtc-XES spectrum of Ti^{III} precursor. In this case in fact, the MOs have mainly O(2s) character and/no little metal contribution and thus cannot be observed.[44] The Kβ" regions of the vtc-XES spectra for Ti^{IV}/SiO_2 and Ti^{III}/SiO_2 are very different from those of the corresponding Ti^{IV} and Ti^{III} precursors, but similar to each other. In particular, in both cases feature A (identifying oxygen ligands) is very intense and broad, whereas feature B (identifying chlorine ligands) is much less visible than in the spectra of the two precursors. Therefore, the Kβ" lines of the vtc-XES spectra provide striking evidence that a ligand exchange takes place when Ti^{IV} and Ti^{III} precursors react with SiO_2: most of the chlorine ligands are substituted by oxygen ligands.

Additional insights can be gained by observing the features that compose the $K\beta_{2,5}$ region of the vtc-XES spectra (grey box in Figure 2c). In general, the $K\beta_{2,5}$ lines are primarily due to transitions involving molecular orbitals having a *p*-type ligand atomic character and therefore they are particularly sensitive to changes in the valence orbitals of the material under investigation.[46,48] In the present case, quantum mechanics calculations (see below and SI) suggest that the $K\beta_{2,5}$ lines are due to transitions involving MOs having either an O(2p)-C(2s2p) character or a Cl(3p) atomic character. Also in this region the spectra of the two precursors are remarkably different from those of the corresponding silica-supported samples, suggesting that the electronic properties and the ligand environment of the Ti sites are changed.

Since the electronic properties of materials are usually the domain of UV-Vis and XANES spectroscopy, we carried out a detailed investigation by means of both techniques. The UV-Vis spectra of the two Ti^{IV} and Ti^{III} chloride tetrahydrofuranates precursors (grey spectra in Figure 3a and b) were already discussed in our previous work.[17,43] Both precursors display a well defined colour: Ti^{IV} is bright yellow, as a consequence of the intense Cl(2p) →Ti(3d) charge-transfer transition having the edge (arbitrarily defined as the maximum of the first derivative) at around 22600 cm^{-1} (2.80 eV). On the contrary, the pale blue colour of Ti^{III} takes origin from the double and well defined d-d absorption band centred around 14000 cm^{-1} (1.74 eV), which is typical of Ti^{III} species (d^1 transition metal) in a six-fold coordination;[51-53] the intense Cl(2p) →Ti(3d) charge transfer falls entirely in the UV region (edge at 26000 cm^{-1}, 3.22 eV). XANES spectroscopy gives complementary information on transitions involving un-occupied states (Figure 3c,d). The XANES spectra of Ti^{IV} and Ti^{III} precursors differ in both the pre-edge and the edge regions. In the pre-edge region, two weak peaks are observed in both cases, which are assigned to 1s → 3pd transitions. These peaks have a lower intensity for the more symmetric Ti^{III} precursor (C_3 symmetry) than for the Ti^{IV} one (C_1 symmetry). The edge position shifts to lower energies by about 2 eV when going from Ti^{III} to Ti^{IV} precursor, as expected on the basis of the formal oxidation state.

Both UV-Vis and XANES spectra of Ti^{IV}/SiO_2 and Ti^{III}/SiO_2 are remarkably different from those of the corresponding precursors. Starting from the UV-Vis spectra (Figure 3a,b), in

both cases the intense edge in the charge-transfer region shifts at higher wavenumbers (*i.e.* the energy necessary for transferring one electron from the ligands to Ti increases); for Ti^{III}/SiO_2 also the absorption bands due to d-d transitions upward shift and broaden. These drastic changes can be qualitatively explained by using the semi-empirical Jorgensen's rules,[54] *i.e.* the energy of a charge-transfer transition is a function of the optical electronegativity values of the metal, $\chi_{opt}(M)$ (which in turns is a function of the metal coordination number), and of the ligand, $\chi_{opt}(X)$, following the equation: $\nu(cm^{-1}) = 30000\ cm^{-1}\ [\chi_{opt}(X)-\chi_{opt}(M)]$. The shift of the charge-transfer band towards higher wavenumber when the Ti precursors are grafted on SiO_2 can be explained by two hypothesis only:[54-56] i) the charge-transfer band is still due to a Cl(2p) →Ti(3d) transition ($\chi_{opt}(X)$ constant), but the Ti sites have now a lower coordination number ($\chi_{opt}(M)$ decreases); or ii) the Ti sites still have a six-fold coordination ($\chi_{opt}(M)$ constant), but a ligand exchange is occurred (from chlorine to oxygen, $\chi_{opt}(X)$ increases). Only the second hypothesis is compatible with the experimental results discussed in above. Therefore, UV-Vis spectroscopy provides an additional evidence that both Ti^{IV} and Ti^{III} precursors do graft to the silica surface by exchanging chlorine ligands with oxygen belonging to the silica surface.

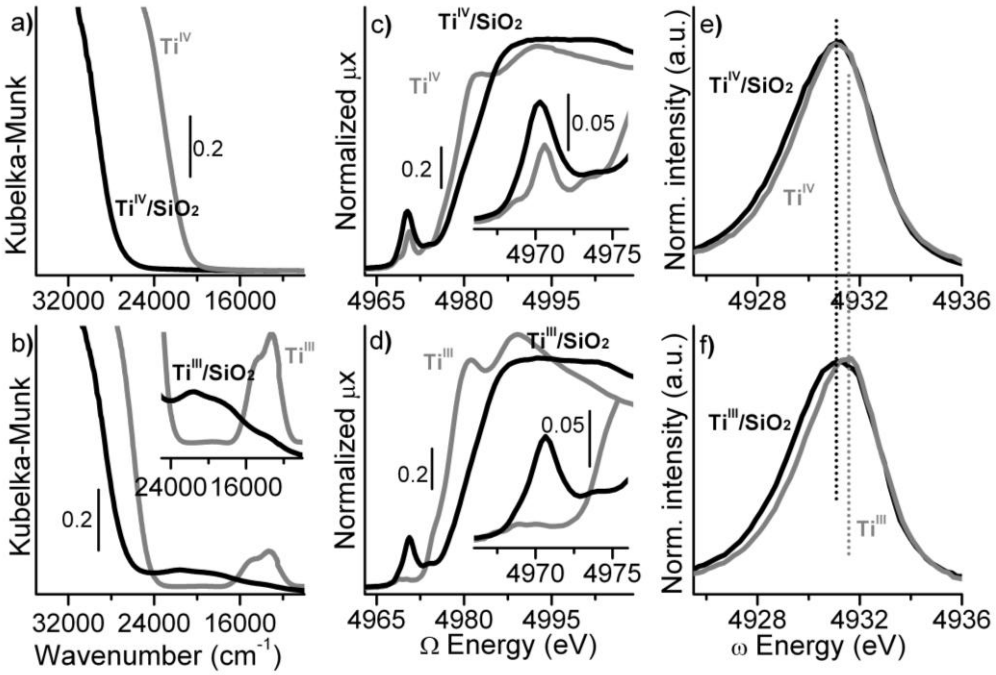

Fig. 3 UV-Vis diffuse reflectance spectra (parts a and b), XANES spectra (parts c and d), and $K\beta_{1,3}$ spectra (parts e and f) for Ti^{IV}/SiO_2 and Ti^{III}/SiO_2 (black spectra) compared to those of the corresponding Ti^{IV} and Ti^{III} precursors (grey); Ti^{IV}: $TiCl_4(thf)_2$; Ti^{III}: $TiCl_3(thf)_3$. Inset in part b) shows an enlargement of the absorption bands in the d-d region. Insets in parts c) and d) display an enlargement of the pre-edge peaks in the XANES spectra.

The evolution of the UV-Vis spectra upon grafting of Ti^{IV} and Ti^{III} precursors on silica is mirrored by the evolution of the XANES spectra, as shown in Figure 3c and d. In both cases: i) the pre-edge peak is enhanced in intensity, suggesting that the supported Ti sites have a six-folded coordination more distorted than that of the Ti precursors; ii) the threshold-edge significantly shifts to higher energy. It is usually difficult to disentangle electronic and geometric information contained in a XANES spectrum. Another method that can be used to characterize the formal oxidation state of 3d-transition-metals is the analysis of the shape and energy position of X-ray emission lines such as $K\alpha_1$, $K\alpha_2$ and $K\beta_{1,3}$, which are less sensitive to the symmetry of the system under investigation compared to XANES.[46,57] It has been shown that $K\alpha_1$, $K\alpha_2$ and $K\beta_{1,3}$ provide similar information, but the $K\beta_{1,3}$ is the line more sensitive to the ligand environment of the metal ion.[58,59] The $K\beta_{1,3}$ spectra of Ti^{IV}/SiO_2 and Ti^{III}/SiO_2 are shown in Figure 3e and f and compared to those of the two precursors. The maxima of the $K\beta_{1,3}$ lines for the two precursors are shifted by about 0.4 eV. No changes are observed in the $K\beta_{1,3}$ spectrum of Ti^{IV}/SiO_2 when compared to that of the corresponding Ti^{IV} precursor. On the contrary, the spectrum of Ti^{III}/SiO_2 is shifted towards low energy with respect to that of Ti^{III}. The energy position of its maximum is close to that of Ti^{IV}/SiO_2, providing evidence that the formal oxidation state of the grafted Ti sites is higher than +3. We propose that the major part of the Ti sites in Ti^{III}/SiO_2 and Ti^{IV}/SiO_2 may have the same formal oxidation number, i.e. +4.

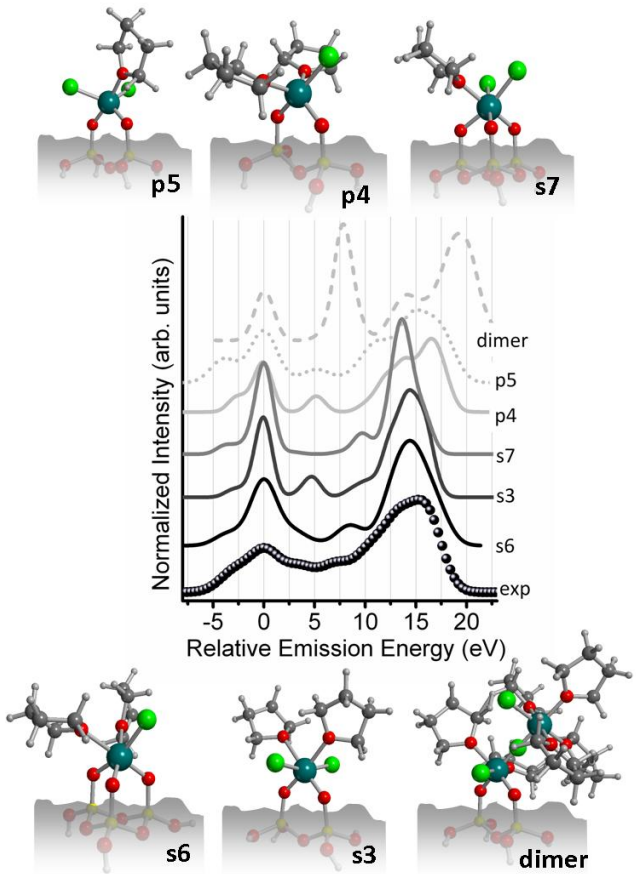

Fig. 4 Experimental XES spectrum of Ti^{IV}/SiO_2 (exp) and selection of spectra simulated by means of the minimal (monomeric) clusters p4, p5, s3, s6, and s7 and of a tentative dimeric model. The labels refer to the names of the clusters reported in Table S3. The spectra have been translated for clarity. In order to evaluate the agreement between the simulated and the experimental vtc-XES spectra the zero of the energy was shifted to the maximum of the Kβ" characteristic of oxygen ligands.

On the basis of the information obtained so far, we carried out a systematic series of theoretical calculations based on ground state density functional theory (section S6), which has been shown to be effective for reproducing the vtc-XES spectral features.[50] We computed all the reasonable monomeric models for the Ti local environment in Ti^{IV}/SiO_2, where Ti is four-, five- and six-folded coordinated, while varying the number of the three possible ligands (*i.e.* oxygen of the silica surface, oxygen of thf and chlorine). It is recalled that the vtc-XES spectrum of Ti^{IV}/SiO_2 is similar to that of Ti^{III}/SiO_2, see Figure 2c. The list of the adopted models is summarized in Table S3 as a function of the Ti coordination number. Also a tentative dimeric model was computed, in order to evaluate the distinctive feature for bridging chlorine ligands. Examples of computed vtc-XES for Ti^{IV}/SiO_2 are shown in Figure 4 in comparison to the experimental spectrum. The relative agreement between the experimental spectrum and the computed ones was evaluated by using a first moment analysis of the experimental vs theoretical features.[29,60] The quality of the calculation is expressed in terms of the quality factor Θ, as discussed in Section S1; the best model corresponds to Θ = 1.0, while the worst has Θ = 4.0. In general, a small Θ value (< 1.5) is obtained for models characterized by a small number of chlorine ligands (maximum 2); the corresponding simulated spectra are shown in Figure 4. In the best model (s6) the Ti site is grafted to the silica surface through three oxygen ligands; the six-fold coordination sphere is completed by two thf and one chlorine ligand. The tentative dimeric model is not able to reproduce the main features of the experimental spectrum, in both Kβ" and $K\beta_{2,5}$ regions. Although the level of calculation could be further improved, and the small models shown in Figure 4 must be taken only as schematic representation of the more complex situation found on amorphous silica, it is evident that vtc-XES spectroscopy coupled with DFT calculation is potentially able to provide structural details on the grafted Ti species.[36]

4. Conclusions

The work reports on a systematic investigation of the structural and electronic properties of silica-supported titanium chloride tetrahydrofuranates samples, obtained by impregnating a polymer-grade dehydroxylated silica with $TiCl_4(thf)_2$ and $TiCl_3(thf)_3$ complexes, precursors of Ziegler-Natta catalysts. While the occurrence of titanium grafting through surface ≡SiOH groups was easily demonstrated by FT-IR spectroscopy, the determination of the local structure of the grafted Ti sites and of their electronic properties required the synergic application of many complementary techniques, coupled with DFT calculations. All the experimental data do suggest that both structural and electronic properties of silica-supported samples are very similar, irrespective of the starting precursor, *i.e.* $TiCl_4(thf)_2$ or $TiCl_3(thf)_3$. In both cases, most of the chlorine ligands originally surrounding the Ti sites are substituted by oxygen ligands upon grafting on silica, as happens for the more reactive and geometrically different $TiCl_4$. The electronic properties of silica-supported Ti sites are largely different from those of the corresponding precursors, and in both cases most of the grafted Ti sites have a formal oxidation state of +4. Besides the interest in Ziegler-Natta catalysis, such investigation could be of high relevance in the field of organometallic chemistry and reactivity of metal-oxide surfaces towards organometallic compounds. The results discussed herein demonstrate that when dealing with the reactivity of molecular complexes towards high surface area amorphous supports care must be taken in analyzing experimental results. In many cases, the observed spectra contain both electronic and geometric information on the supported metal sites, and it is often difficult to disentangle the two. The synergic use of complementary experimental technique is a valuable instrument to get insights into the properties of the grafted sites.[43]

Ackowedgments

We would like to thank Prof. A. Zecchina for the everyday discussion and for his fruitful contribution to spectroscopy over the years. We are grateful to Olivier Mathon (BM23 at ESRF), Mauro Rovezzi and Christophe Lapras (ID26 at ESRF) for the technical help during the XAS/XES experiment, and to Harald Muller (Chemical Lab at ESRF) for providing us the indispensable (and always perfect) glove-box during the experiments at ESRF.

Notes and references

[a] *Department of Chemistry, NIS Centre of Excellence and INSTM University of Torino, via Quarello 15, I-10135 Torino, Italy. Fax: (+) 39 011 6707855; Tel. (+) 39 011 6708373; E-mail: elena.groppo@unito.it*

[b] *European Synchrotron Radiation Facility, 6 Rue Jules Horowitz, 38043 Grenoble, France*

[c] *Institut Laue Langevin, 6 Rue Jules Horowitz BP 156, F-38042 Grenoble Cedex 9, France*

[d] *Centro Ricerche per le Energie non Convenzionali, Istituto ENI Donegani, Via Fauser,4 - 28100 Novara, Italy*

† Electronic Supplementary Information (ESI) available: additional experimental details, XRPD patterns, FT-IR data of interaction with H_2O and CO as probe molecules, details on EXAFS and vtc-XES dta analysis. See DOI: 10.1039/b000000x/

1 Basset, J. M.; Lefebvre, F.; Santini, C. *Coord. Chem. Rev.* 1998, **180**, 1703.

2 Coperet, C.; Chabanas, M.; Saint-Arroman, R. P.; Basset, J. M. *Angew. Chem.-Int. Edit.* 2003, **42**, 156.

3 Rascon, F.; Wischert, R.; Coperet, C. *Chem. Sci.* 2011, **2**, 1449.

4 Gajan, D.; Coperet, C. *New J. Chem.* 2011, **35**, 2403.

5 Amor Nait Ajjou, J.; Scott, S. L. *Organometallics* 1997, **16**, 86.

6 Demmelmaier, C. A.; White, R. E.; van Bokhoven, J. A.; Scottt, S. L. *J. Phys. Chem. C* 2008, **112**, 6439.

7 Zhuravlev, L. T. *Colloid Surf. A* 2000, **173**, 1.

8 Thomas, J. M.; Raja, R.; Lewis, D. W. *Angew. Chem.-Int. Edit.* 2005, **44**, 6456.

9 Pullukat, T. J.; Hoff, R. E. *Catal. Rev.-Sci. Eng.* 1999, **41**, 389.

10 McDaniel, M. P. *Adv. Catal.* 2010, **53**, 123.

11 Groppo, E.; Lamberti, C.; Bordiga, S.; Spoto, G.; Zecchina, A. *Chem. Rev.* 2005, **105**, 115.

12 Zecchina, A.; Groppo, E. *Proc. R. Soc. A-Math. Phys. Eng. Sci.* 2012, **468**, 2087.

13 Gianolio, D.; Groppo, E.; Vitillo, J. G.; Damin, A.; Bordiga, S.; Zecchina, A.; Lamberti, C. *Chem. Commun*. 2010, **46**, 976.

14 Groppo, E.; Lamberti, C.; Spoto, G.; Bordiga, S.; Magnacca, G.; Zecchina, A. *J. Catal.* 2005, **236**, 233.

15 Hlatky, G. G. *Chem. Rev.* 2000, **100**, 1347.

16 Lee, M. Y.; Scott, S. L. *Chem.-Eur. J.* 2011, **17**, 4632.

17 Seenivasan, K.; Sommazzi, A.; Bonino, F.; Bordiga, S.; Groppo, E. *Chem. Eur. J.* 2011, **17**, 8648.

18 Morrow, B. A.; Hardin, A. H. *J. Phys. Chem.* 1979, **83**, 3135.

19 Kinney, J. B.; Staley, R. H. *J. Phys. Chem.* 1983, **87**, 3735.

20 Haukka, S.; Lakomaa, E. L.; Jylha, O.; Vilhunen, J.; Hornytzkyj, S. *Langmuir* 1993, **9**, 3497.

21 Haukka, S.; Lakomaa, E. L.; Root, A. *J. Phys. Chem.* 1993, **97**, 5085.

22 Kytokivi, A.; Haukka, S. *J. Phys. Chem. B* 1997, **101**, 10365.

23 Schrijnemakers, K.; Van Der Voort, P.; Vansant, E. F. *Phys. Chem. Chem. Phys.* 1999, 2569.

24 Bini, F.; Rosier, C.; Saint-Arroman, R. P.; Neumann, E.; Dablemont, C.; de Mallmann, A.; Lefebvre, F.; Niccolai, G. P.; Basset, J. M.; Crocker, M.; Buijink, J. K. *Organometallics* 2006, **25**, 3743.

25 Tosin, G.; Santini, C. C.; Taoufik, M.; De Mallmann, A.; Basset, J. M. *Organometallics* 2006, **25**, 3324.

26 Saint-Arroman, R. P.; Basset, J. M.; Lefebvre, F.; Didillon, B. *Appl. Catal. A-Gen.* 2005, **290**, 181.

27 Le Roux, E.; Chabanas, M.; Baudouin, A.; de Mallmann, A.; Coperet, C.; Quadrelli, E. A.; Thivolle-Cazat, J.; Basset, J. M.; Lukens, W.; Lesage, A.; Emsley, L.; Sunley, G. J. *J. Am. Chem. Soc.* 2004, **126**, 13391.

28 Bordiga, S.; Groppo, E.; Agostini, G.; Van Bokhoven, J. A.; Lamberti, C. *Chem. Rev.* 2013, **113**, 1736.

29 Glatzel, P.; Bergmann, U. *Coord. Chem. Rev.* 2005, **249**, 65.

30 Schoonheydt, R. A. *Chem. Soc. Rev.* 2010, **39**, 5051.

31 Manxzer, L. E. *Inorg. Synth.* 1982, **21**, 135.

32 Manxzer, L. E. *Inorg. Synth.* 1982, **21**, 137.

33 Ravel, B.; Newville, M. *J. Synchrot. Radiat.* 2005, **12**, 537.

34 Zabinsky, S. I.; Rehr, J. J.; Ankudinov, A. L.; Albers, R. C.; Eller, M. J. *Phys. Rev. B* 1995, **52**, 2995.

35 Gallo, E.; Lamberti, C.; Glatzel, P. *Phys. Chem. Chem. Phys.* 2011, **13**, 19409.

36 Gallo, E.; Bonino, F.; Swarbrick, J. C.; Petrenko, T.; Piovano, A.; Bordiga, S.; Gianolio, D.; Groppo, E.; Neese, F.; Lamberti, C.; Glatzel, P. *ChemPhysChem* 2013, **14**, 79.

37 Neese, F. *Wiley Interdiscip. Rev.-Comput. Mol. Sci.* 2012, **2**, 73.

38 Bordiga, S.; Roggero, I.; Ugliengo, P.; Zecchina, A.; Bolis, V.; Artioli, G.; Buzzoni, R.; Marra, G.; Rivetti, F.; Spano, G.; Lamberti, C. *J. Chem. Soc. Dalton Trans.* 2000, 3921.

39 Bordiga, S.; Ugliengo, P.; Damin, A.; Lamberti, C.; Spoto, G.; Zecchina, A.; Spano, G.; Buzzoni, R.; Dalloro, L.; Rivetti, F. *Top. Catal*. 2001, **15**, 43.

40 Ricchiardi, G.; Damin, A.; Bordiga, S.; Lamberti, C.; Spano, G.; Rivetti, F.; Zecchina, A. *J. Am. Chem. Soc.* 2001, **123**, 11409.

41 Grau, E.; Lesage, A.; Norsic, S.; Copéret, C.; Monteil, V.; Sautet, P. *ACS Catal.* 2013, **3**, 52.

42 Groppo, E.; Prestipino, C.; Cesano, F.; Bonino, F.; Bordiga, S.; Lamberti, C.; Thüne, P. C.; Niemantsverdriet, J. W.; Zecchina, A. *J. Catal*. 2005, **230**, 98.

43 Groppo, E.; Seenivasan, K.; Barzan, C. *Catal. Sci. Technol.* 2013, **3**, 858.

44 Swarbrick, J. C.; Kvashnin, Y.; Schulte, K.; Seenivasan, K.; Lamberti, C.; Glatzel, P. *Inorg. Chem.* 2010, **49**, 8323.

45 Smolentsev, G.; Soldatov, A. V.; Messinger, J.; Merz, K.; Weyhermuller, T.; Bergmann, U.; Pushkar, Y.; Yano, J.; Yachandra, V. K.; Glatzel, P. *J. Am. Chem. Soc.* 2009, **131**, 13161.

46 Bergmann, U.; Horne, C. R.; Collins, T. J.; Workman, J. M.; Cramer, S. P. *Chem. Phys. Lett.* 1999, **302**, 119.

47 Glatzel, P.; Weng, T.-C.; Kvashnina, K.; Swarbrick, J.; Sikora, M.; Gallo, E.; Smolentsev, N.; Mori, R. A. *J. Electron Spectrosc. Relat. Phenom.* 2012, http://dx.doi.org/10.1016/j.elspec.2012.09.004.

48 Pizarro, S. A.; Glatzel, P.; Visser, H.; Robblee, J. H.; Christou, G.; Bergmann, U.; Yachandra, V. K. *Phys. Chem. Chem. Phys.* 2004, **6**, 4864.

49 Lee, N.; Petrenko, T.; Bergmann, U.; Neese, F.; DeBeer, S. *J. Am. Chem. Soc.* 2010, **132**, 9715.

50 Lancaster, K. M.; Roemelt, M.; Ettenhuber, P.; Hu, Y.; Ribbe, M. W.; Neese, F.; Bergmann, U.; DeBeer, S. *Science* 2012, **334**, 974.

51 Clark, R. J. H.; Lewis, D.; Machin, D. J.; Nyholm, R. S. *J. Chem. Soc.* 1963, 379

52 Clark, R. J. H. *J. Chem. Soc.* 1964, 417.

53 Brisdon, B. J.; Ozin, G. A.; Walton, R. A. *J. Chem. Soc. A* 1969, 342.

54 Jorgensen, C. K. *Progr. Inorg. Chem.* 1970, **12**, 101.

55 Jorgensen, C. K., *Halogen Chemistry*; Academic Press: New York, **1967**; Vol. 1.

56 Crouch, P. C.; Fowles, G. W. A.; Walton, R. A. *J. Chem. Soc. A* 1969, 972.
57 Peng, G.; Degroot, F. M. F.; Hamalainen, K.; Moore, J. A.; Wang, X.; Grush, M. M.; Hastings, J. B.; Siddons, D. P.; Armstrong, W. H.; Mullins, O. C.; Cramer, S. P. *J. Am. Chem. Soc.* 1994, **116**, 2914.
58 Glatzel, P.; Smolentsev, G.; Bunker, G. *J. Phys.: Conf. Series* 2009, **190**, 012046.
59 Vanko, G.; Neisius, T.; Molnar, G.; Renz, F.; Karpati, S.; Shukla, A.; de Groot, F. M. F. *J. Phys. Chem. B.* 2006, **110**, 11647.
60 Glatzel, P.; Sikora, M.; Smolentsev, G.; Fernandez-Garcia, M. *Catal. Today* 2009, **145**, 294.